CHAPTER 3
TOPOGRAPHY

The topography (or morphology) of a mountain belt reflects the combined effects of climatic, magmatic, and tectonic processes. Tectonic processes, i.e. vertical and horizontal displacements of rock, and magmatic processes (i.e. volcanism) construct topography and are driven by endogene dynamics. In contrast, surface processes like erosion destruct topography and are driven by exogene dynamics, for instance climate. Montgomery et al. (2001) concluded from a large-scale (continental scale) topographic analysis of the Andes that hemisphere-scale climatic variations (beside tectonic variations, Isacks, 1988) are a first-order control on the morphology of the Andes. They showed that major morphologic features like hypsometry and maximum elevation correlate with climatic regimes in the Andes.

In this chapter, the focus is on the morphology of the Andes at the transition from the high and "dry" Central Andes to the low and "wet" Southern Andes between latitudes 37° and 43°S to verify the hypothesis of Montgomery et al. (2001) at a smaller scale but with a higher resolution. I.e., a 50 m-DEM has been used with respect to the 1 km-DEM used by Montgomery et al. (2001). The results support the ideas of Montgomery et al. (2001) that latitudinal morphologic gradients correlate with climatic gradients. In addition, when compared with the exhumation pattern determined by thermochronologic (Gräfe, pers. comm.) and geothermobarometric (Seifert et al., in press) studies, the morphometric results strongly suggest that climatic factors not only control the morphology of the Main Cordillera but also have significant control on exhumation in the Southern Andes. At the end of this chapter, the mechanisms of erosion and uplift are discussed. Geomorphometric data are reported in Appendix IV, Tab. A3.

3.1 Swath profiles

Swath profiles along (N-S) and across (E-W) the watershed, which are based on the digital average topographic map (Ch. 2.2.3) and base level map (Ch. 2.2.4), show the general topographic features of this mountain belt (Fig. 3.1). The average topography map shows the smoothed topography and thus is suitable for recognizing broader geomorphic features. The base level map shows the minimum elevation and reflects the average depth of river incision, i.e. the foot of the mountain belt. The profiles represent an area of 1000 x 1 km (N-S) and 250 x 1 km (E-W).

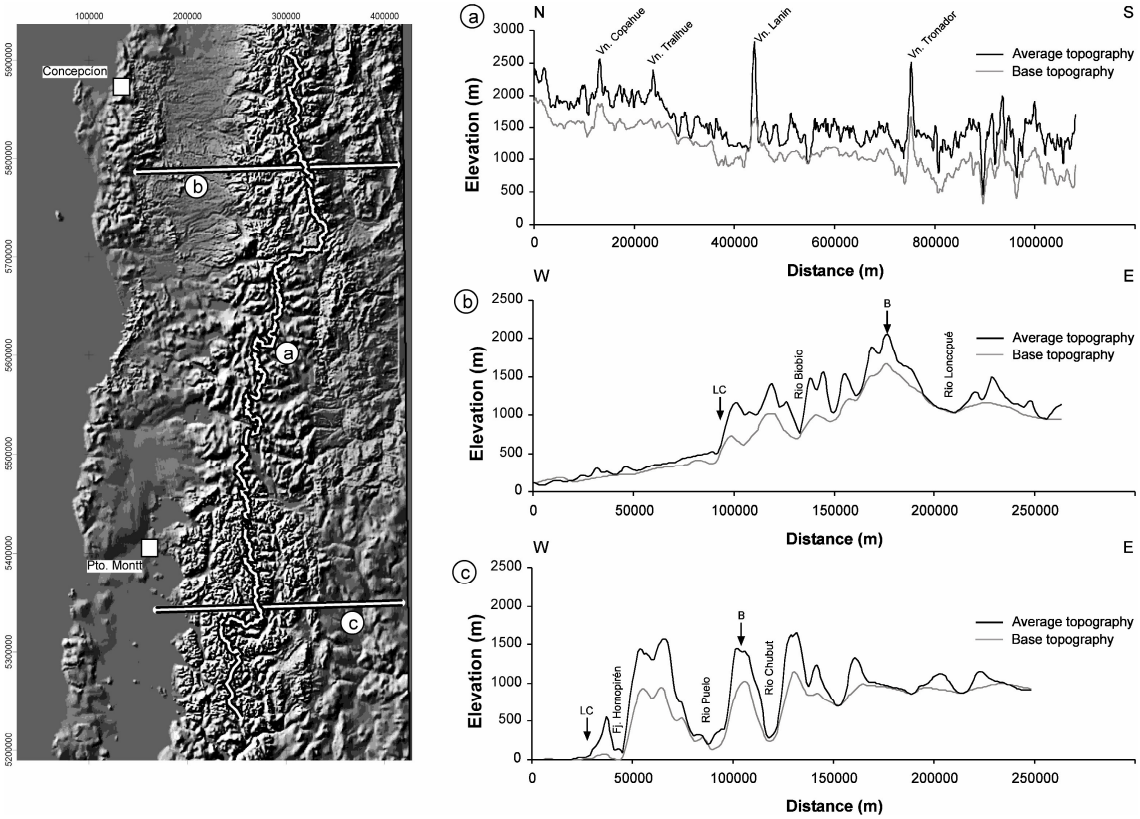

Fig. 3.1: *Profiles along (a) and across (c, d) the Southern Andean Main Cordillera.*

3.1.1 Along-watershed profile (N-S)

The N-S profile (Fig. 3.1a) runs from 37°S to 43°S along the watershed of the study area which forms the political border of Chile and Argentina. It indicates a general southward decreasing elevation of the cordillera coeval with a southward increasing local relief (i.e., the difference in elevation between the average topography and the base level). Peaks in the average topography correspond to quaternary stratovolcanoes, from north to south: Vn. Nevados de Chillan, Vn. Copahue, Vn. Tralihue, Vn. Lanin, and Vn. Tronador. In the northern part, between Vn. Nevados de Chillan and Vn. Tralihue (0 – 240 km profile length starting in the north), the profile is located on top of the Pino Hachado High, a Pliocene lava plateau with an average elevation of ca. 2000 m and a base level of ca. 500 m. South of Vn. Tralihue, the profile descend from the Pino Hachado High by ca. 400 m altitude. In the central part, between the Pino Hachado High and Vn. Tronador volcano (240 – 750 km profile length), the profile is located on top of dominantly granitoid basement which shows a regular southward slope decreasing from ca. 1600 m to 1300 m. The base level decreases consistently from around 1300 m to 1000 m. In the southern part, south of Vn. Tronador (750 – 1000 km profile length), the profile is located on top of granitoid basement which rises up to 1900 m but is generally around 1500 m. The base level is at ca. 900 m indicating a

higher local relief (ca. 600 - 1000 m) in this part of the profile with respect to the northern part (300 – 400 m).

3.1.2 Cross-cordillera profiles (E-W)

E-W profiles cross the cordillera at 38°S (Fig. 3.1b) and at 42°S (Fig. 3.1c) between 70°W and 73°W. Both profiles indicate asymmetric mountain belt geometry with low local relief/low altitude foreland basin (the Longitudinal Valley) to the west and a low local relief hinterland which is in average at a higher elevation than the foreland and therefore referred to as a "highland"-hinterland.

The northern cross-cordillera profile (38°S, Fig. 3.1b) shows that the longitudinal basin, which in this area is filled with volcanoclastic material of the Pliocene Fm. Malleco, has a wedge shape with a surface rising from ca. 100 m in the west to ca. 550 m at the transition to the cordillera (labeled LC = Longitudinal Valley-Main Cordillera transition in Fig. 3.1). The cordillera itself rises abruptly at the LC by ca. 600 m where granitoid basement makes up the foothills of the cordillera. This abrupt change in elevation may reflect tectonic uplift of the cordillera with respect to the Longitudinal Valley along either an east-dipping inverse fault or west-dipping normal fault. To the east of LC, the profile shows a more gradual elevation increase to ca. 2000 m at the watershed (labeled B = political border in Fig. 3.1) which is located on top of the Pino Hachado High, a Pliocene lava plateau. To the east of B, the elevation decreases rapidly down to 1000 - 1200 m and remains relatively constant further east forming a weakly dissected highland-like hinterland. The local relief is highest (400 – 600 m) in the part of the cordillera west of the watershed (B) where V-shaped river valleys (e.g. the Biobío river valley) occur. The cordillera in this part shows a high-frequency low-amplitude relief.

The southern cross-cordillera profile (42°S, Fig. 4.1c) gives no information about the topography of the Longitudinal Valley because it is below sea level (Golfo de Ancud). Here, the Main Cordillera rises from sea level to ca. 1400 m average topography within a distance of ca. 28 km. To the east of this topographic step, which may represent either an east-dipping inverse fault or west-dipping normal fault, a number of more or less concordant peaks with average elevations of ca. 1500 m, separated by deeply eroded U-shaped glacial valleys occur over a length of ca. 80 km. The average relief in this low-frequency high amplitude part of the cordillera is considerably high ranging between 400 – 800 m. To the east, the elevation drops to ca. 1000 m and remains at this value to the east forming a weakly dissected highland-hinterland.

3.1.3 Interpretation

The marked asymmetry of the Main Cordillera with a deeply dissected western part and a relatively less dissected highland-hinterland basically reflects the climatic pattern of the study area where westerly winds focus erosion on the western part of the mountain belt. The southward increasing local relief and the change from V-shaped valleys in the north to U-shaped valleys in the south indicate a southward change from fluvial to glacial erosion processes.

3.2 Relief distribution

After having recognized the broad morphologic features of the Southern Andean Main Cordillera, the focus is now on the windward, western flank of the Main Cordillera where erosion is localized. The study area has been divided into six subareas, each spanning one degree latitude from the water divide to the eastern border of the Longitudinal Valley (Fig. 3.2). The transition from the Main Cordillera to the Longitudinal Valley is defined on the base of geomorphology (change from higher to lower slopes) and geology (change from dominantly Tertiary volcano-sedimentary rocks overlying a granitoid basement in the Main Cordillera to Quaternary deposits in the Longitudinal Valley). The mean, minimum, and maximum elevation and the distribution (frequency) of elevations in each subarea have been calculated from the 50 m-DEM (Fig. 3.3).

3.2.1 Maximum, minimum, and mean elevation

From north to south, the mean elevation of the Main Cordillera decreases from above 1100 m in area 1 and 2 to less than 700 m in area 6 (Fig. 3.3 a). Accordingly, the minimum elevation (which is the elevation of the Longitudinal Valley-Main Cordillera transition) falls from around 230 m in areas 1 and 2 below sea level in areas 5 and 6. Due to large volcanic edifices in areas 3 and 5 (Vn. Lanin and Vn. Tronador, respectively), the maximum elevation varies significantly along strike of the study area but show clearly a tendency to fall to the south: If considering only the areas without large volcanoes, i.e. areas 1, 2, 4, and 6, the maximum elevation decreases from values around 3500 m in the north to around 2400 m in the south.

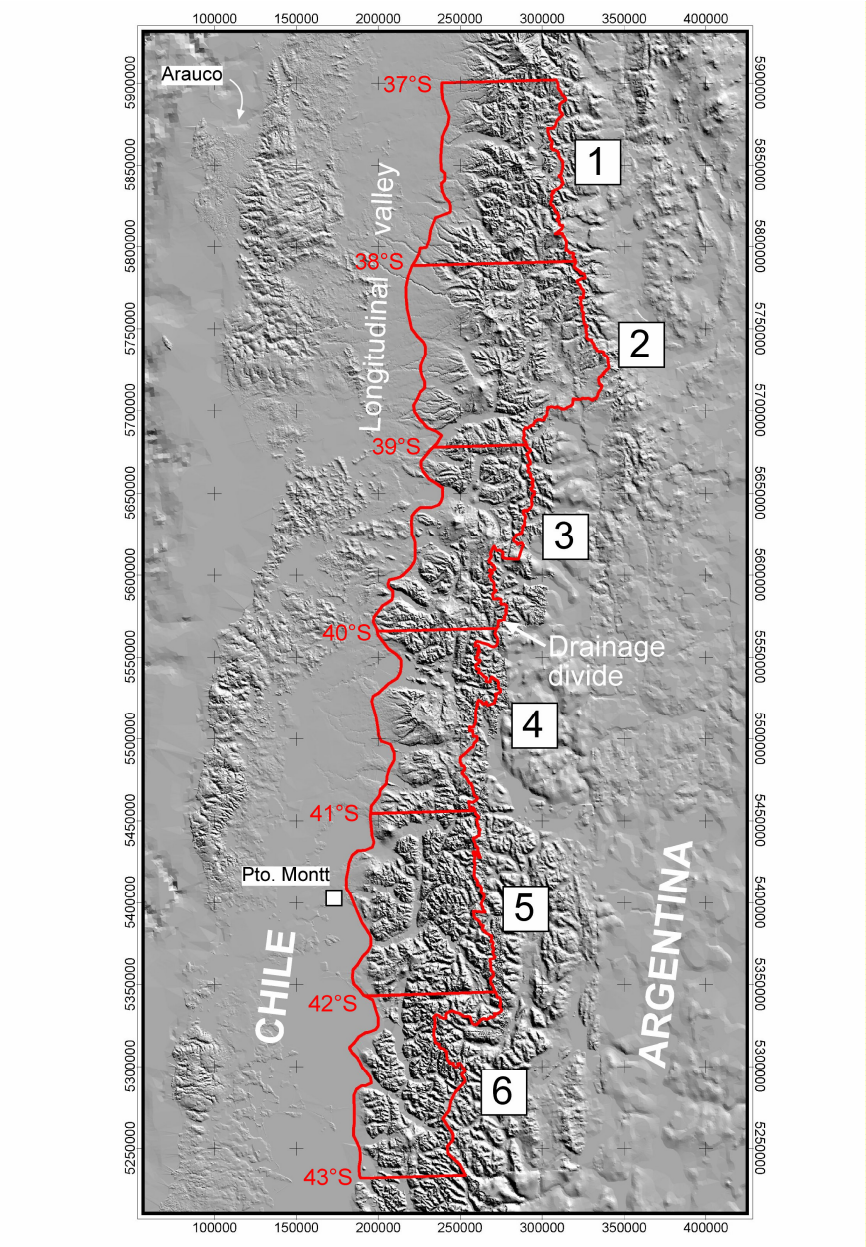

Fig. 3.2: *Subareas used for terrain analysis (UTM 19 S projection, PSAD 1956 ellipsoid).*

3.2.2 Modal elevation

Consistent trends are visible from the area-altitude diagram (Fig. 3.3 b) which gives information about the modal elevation (the elevation with the greatest frequency in the landscape). All curves show a bimodal distribution which reflects the significant amount of lowland rivers and lakes beside uplifted areas and volcanic plateaus characterizing the Southern Andean landscape. Low- and upland modal elevations are, respectively, around 400 m and 1500 m in areas 1 and 2, around 250 m and 1250 m in areas 3 and 4, and around sea level and 900 m in areas 5 and 6.

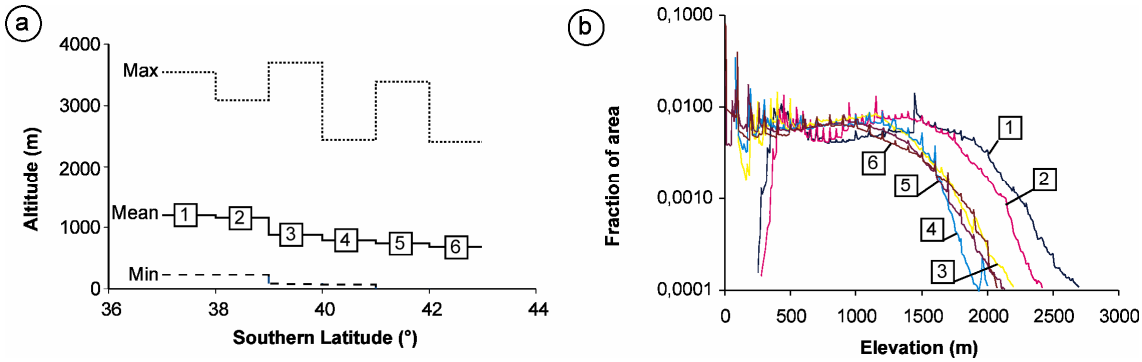

Fig. 3.3: *Relief distribution: (a) Along-strike variation of maximum, minimum, and mean elevation, (b) elevation frequency plot.*

3.2.3 Interpretation

The southward decrease of mean, modal, minimum, and maximum elevations may be interpreted either as an effect of the climatic gradient (more erosion in the south) or as an effect of different tectonic regimes (more tectonic uplift in the north). However, to assess the relative importance of climate and tectonics for the development of Southern Andean topography more information on the spatial and temporal variation of erosion and tectonics is needed. To further constrain the impact of erosion along the Main Cordillera, hypsometric and slope analyses have been performed, the results of which are reported in the following sections.

3.3 Hypsometry

Hypsometric analysis (or area-altitude analysis) is the study of the distribution of horizontal cross-sectional area of a landmass with respect to elevation (Strahler, 1952). Classically, hypsometric analysis has been used to differentiate between erosional landforms at different stages during their evolution (Strahler, 1952, Schumm, 1956). The hypsometric integral I is the area beneath the curve which relates the percentage of total relief to cumulative percent of area. This provides a measure of the distribution of landmass volume remaining beneath or above a basal reference plane. Hypsometric curves and integrals can be interpreted in terms of degree of basin dissection and relative landform age: Convex-up curves with high integrals are typical for youth, undissected (disequilibrium stage) landscapes; smooth, s-shaped curves crossing the center of the diagram characterize mature (equilibrium stage) landscapes, and concave-up with low integrals typify old and deeply dissected landscapes (Strahler, 1952). Strahler (1952) found also that the hypsometric integral is inversely correlated with total

relief, slope steepness, drainage density and channel gradients. These parameters would be expected to correlate positively with rates of erosion. One might thus expect that in areas with similar rock type and tectonics, the hypsometric integral would also correlate inversely with erosion.

3.3.1 Derivation of hypsometry

Hypsometric data were derived for each of the 6 subareas of Fig. 3.2 from the 50 m-DEM. The percentage hypsometric method used here relates the area enclosed between a given contour and the basal plane of the analyzed area to the height of that contour above the basal plane. Two ratios are involved and plotted against each other on a diagram: the abscissa represents the ratio of area between a given contour and the basal plane (cumulative area), the ordinate represents the ratio of height of a given contour above the basal plane to the total height of the area (proportion of height). The resulting hypsometric curve permits comparison of areas of different sizes and elevations. It expresses the manner in which the volume above the basal plane is distributed from base to top. Hypsometric curves always originate in the lower left-hand corner and reach the upper right-hand corner. It may, however, take any one of a variety of paths between these points, depending upon the distribution of the landmass from base to top. Integration of the hypsometric curve gives the hypsometric integral I. Pike and Wilson (1971) proved mathematically that the elevation-relief ratio E which is defined as

E = (mean elevation – minimum elevation)/(maximum elevation – minimum elevation)

is identical to the hypsometric integral I but has the advantage that it is much more easy to obtain numerically. In this work, E is therefore used instead of I.

3.3.2 Results and interpretation

Fig. 3.4 shows the results of hypsometric analysis for the 6 subareas. Hypsometric curves show all a very straight shape and low hypsometric integrals/elevation-relief ratios indicating a mature (equilibrium stage) landscape. A common feature of all curves is a “shoulder” on the right side of the diagram. This shoulder reflects a landmass distribution where the major volume is at relatively low elevations. In the study area, more than 80 % of area (or volume) lay at elevations less than half of the respective maximum elevation.

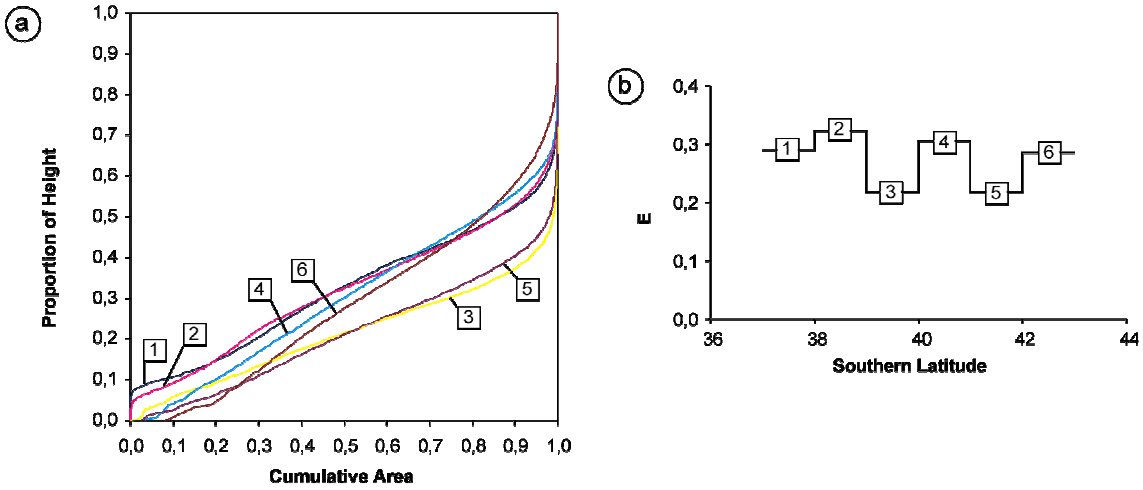

Fig. 3.4: *Hypsometry of the Southern Andes: (a) Hypsometric curves, (b) along-strike variation of elevation-relief ratio.*

Montgomery et al. (2001) found similar hypsometric curves when analyzing the 1-km DEM. They interpreted the characteristic shoulder in the hypsometry as a result of glacial processes, which preferentially erode higher parts of the cordillera. If this idea is valid, one should expect that the development of a shoulder in the hypsometry should correlate with other morphometric parameters indicative of glacial erosion, for example with modal and mean elevation (previous chapter) and slope and roughness (following chapters). This is not the case: The hypsometric shoulder is a common feature of all areas. In contrast, mean and modal elevations continuously decreases to the south whereas mean slope and roughness increase to the south as an effect of increasing dominance of glacial processes. Another possibility to create a shoulder in the hypsometry is to create high peaks standing above a surface. Indeed, subareas 3 and 5, where the shoulder is most pronounced, include the highest volcanoes of the study area, i.e. the 3776 m high Vn. Lanin at ca. 39.6°S and the 3554 m high Vn. Tronador at ca. 41.2°S, respectively. Thus it is suggested that the hypsometric shoulder is a consequence of high altitude stratovolcanoes of the Southern Volcanic Zone of the Andes.

3.4 Roughness

The roughness of a landscape describes how deep and narrow it is dissected by erosion. In this way, it is correlated proportional with the hypsometric integral and the elevation-relief ratio. Slope angles and the surface ratio are measures of roughness.

3.4.1 Slope distribution

Slope angles were calculated for each of the 6 subareas in Fig. 3.2 from the 50 m-DEM. The slope for each cell was calculated from the 9 neighboring cells according to the average maximum technique (Burrough, 1986).

Fig. 3.5 displays the results of the slope analysis. In the slope frequency plot (Fig. 3.5 a), the ordinate represents the fraction of area with a certain slope given on the abscissa. There is a tendency towards lower slopes in the northern part of the study area with respect to the southern area: Areas 1 to 4 are dominated by near flat area as indicated by the high fraction of area with slope angles smaller than 5-10°. These flat areas are Pliocene to Quaternary plateau lavas (e.g., Fm. Malleco, Fm. Cola de Zorro), lakes and flat bottomed valleys. In contrast, the areas 5 and 6 show a broader slope distribution with a peak at 0° representing lakes and fjords and a plateau-like slope distribution up to 30° slope angle. Mean slopes are around 13° in areas 1 – 4 and significantly higher with values around 19° in areas 5 and 6 (Fig. 3.5 b).

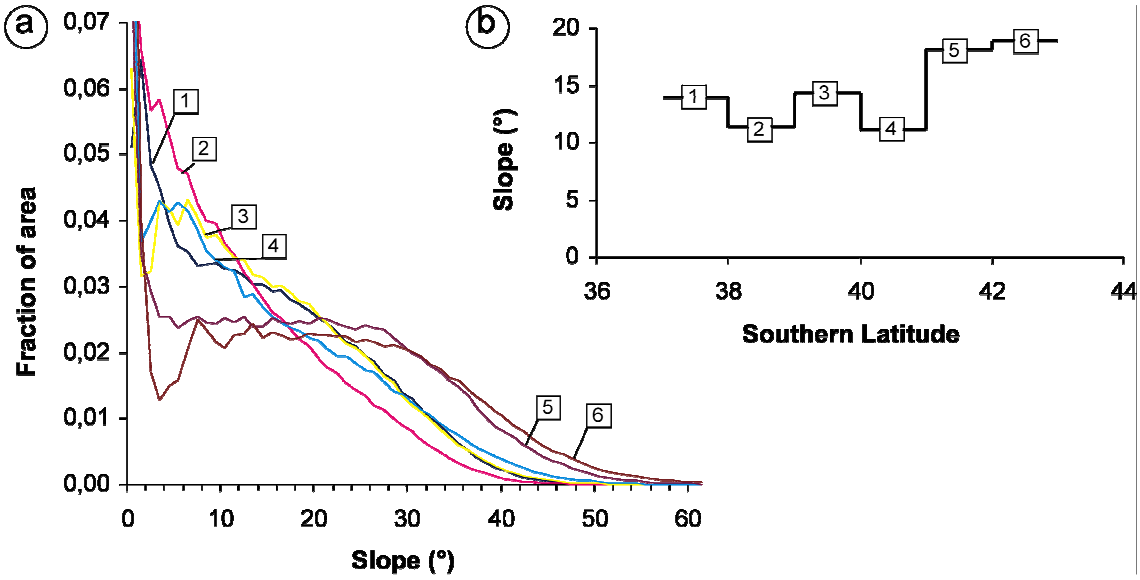

Fig. 3.5: *Slope distribution in the Southern Andes: a) Slope frequency plot, b) Mean slope versus southern latitude.*

3.4.2 Surface ratio

The surface ratio is defined as the ratio between the surface area and the planimetric area. The surface ratio was calculated from the 50 m-DEM for each of the 6 subareas in Fig. 3.2.

Fig. 3.6 shows the results of surface ratio calculation. Surface ratios increases from north to south from values around 1.05 in subarea 1 to 1.11 in subarea 6.

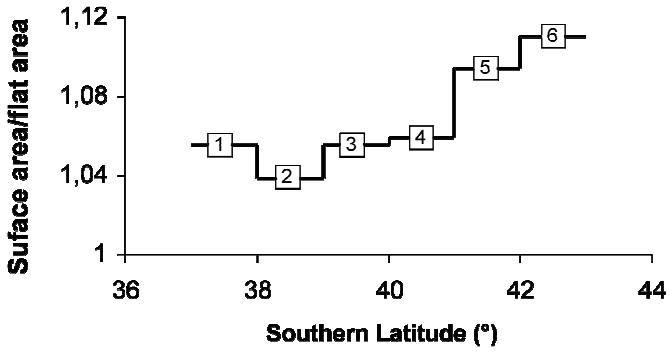

Fig. 3.6: *Variation of surface ratio.*

3.4.3 Interpretation

Slope analysis and surface ratio calculation both indicate a southward increasing roughness and consequently a greater dissection of the landscape in the study area. This is consistent with the hypothesis that the southern parts of the study area were affected by glacial erosion since this mechanism leads generally to deeply dissected landscapes. In contrast to the hypsometric integral, the surface ratio is not affected by the existence of high volcanoes in subareas 3 and 5.

3.5 Discussion

3.5.1 Spatial and temporal variation of erosion

Along strike of the mountain belt this analysis revealed significant topographic gradients, i.e., southward decreasing elevation accompanied by southward increasing dissection. Obviously, these gradients can be explained by southward increasing significance of erosion. Today, glaciers are found exceptionally on top of volcanoes

between 35° and 41°S, cirque glaciers are found south of 41°S as well (Lliboutry, 1999). However, probably up to 40 glaciations have taken place in Patagonia during the last 7 Ma (Mercer and Sutter, 1982, Rabassa and Clapperton, 1990, Lliboutry, 1956, 1999), with the last one (the Llanquihue event 20 ka ago, Mercer, 1976, Heusser, 1990) being the second most extensive after the greatest glaciation (1.2 Ma ago, Mercer, 1976). During both, the last and the greatest glaciations, large ice caps covered the Main Cordillera south of ca. 40°S, the ice front reached the western coast of the continent south of ca. 42°S (Bangs and Cande, 1997). To the north, moraine systems occur within the Longitudinal Valley and northward successively higher parts of the Main Cordillera (Rabassa and Clapperton, 1990, and references therein) indicating that glacial processes were restricted to higher parts of the Main Cordillera north of ca. 40°S.

The change of erosion mechanism from fluvial to glacial along strike of the Main Cordillera should result in a significant change in magnitudes and rates of erosion and exhumation. Longterm rates of erosion (operating over 10^3 to 10^6 years) may reach values of ca. 10 mm/a in catchment areas comparable with those investigated here (3000 - 7000 km^2) if glacial processes dominate. If fluvial processes dominate, erosion may reach values between 0.1 and 1 mm/a (Hallet et al., 1996). Since glaciation started ca. 7 Ma ago in the Southern Andes (Mercer and Sutter, 1982), erosion should theoretically have been able to thin the crust by several tens of kilometers in the southern part of the study area where glacial erosion have occurred. In the northern part of the study area, where fluvial processes have dominated, only several hundreds of meters to a few kilometers may have been eroded. This is consistent with magnitudes, rates and time lengths of exhumation indicated by geothermobarometric and thermochronologic data in the study area: Apatite fission track ages (Gräfe, pers. comm.) suggest exhumation at rates up to 50°C/Ma (ca. 1 - 2 mm/a) during the past million years. Al-in-hornblende data (Seifert et al., in press) indicate post-Miocene erosion levels of less than 3 km in the north and up to 15 km in the south.

To investigate the spatial and temporal correlation of erosion and exhumation in more detail, their relationship with topography has been investigated using the hypsometry to calculate the changes in surface area above the glacial equilibrium line altitude (ELA). The ELA is the altitude on a glacier at which annual accumulation is exactly matched by annual ablation, so that the net mass balance for the glacier is zero. Since the ELA forms an upper envelope on the development of topography through which only a relatively small amount of material is allowed to pass (Brozovic et al., 1997), an increasing amount of area above the ELA would increase the rates of ice flux and consequently the rates of erosion and exhumation.

The current snowline can be used as a proxy for the actual regional ELA (Brozovic et

al., 1997). It has been derived by analysis of Landsat TM images (Ch. 2.2.5) and decreases linearly with -250m/°S from ca. 2250 m in subarea 1 (37 – 38°S) to around 750 m in subarea 6 (42 – 43°S).

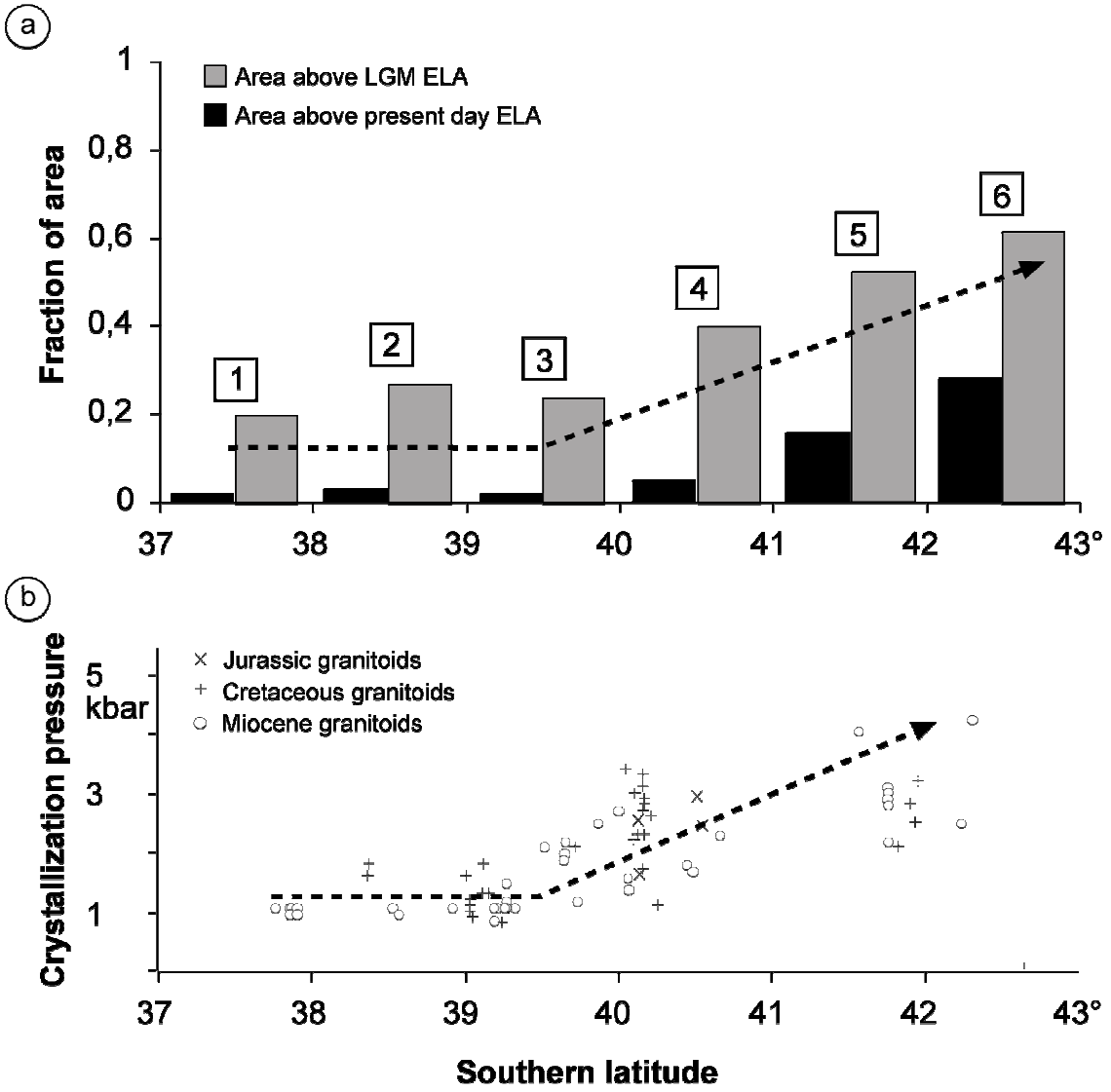

Fig. 3.7: *Erosion and exhumation in the Southern Andes: a) Along-strike change of glaciated area. Abbreviations: ELA = equilibrium line altitude, LGM = last glacial maximum. b) Along strike exhumation pattern indicated by crystallization depths of granitoids of the NPB inferred from Al-in-hbl geothermobarometry (data from Seifert et al., in press).*

As is obvious from Fig. 3.7 a, a southward linear decrease of the ELA results in a non-linear increase of glaciated area: Between 37° and 40°S, less than 3% of the landscape is above the snowline today. South of 40°S, the area above the actual ELA increases constantly up to ca. 30%. This abrupt increase in glaciated area south of 40°S is correlated with the along-strike exhumation pattern (Fig. 3.7 b): Between 37° and 40°S, the depth of exhumation is generally lower than ca. 3 - 6 km as indicated by

crystallization pressures below 1 - 2 kbar, whereas south of 40°S, exhumation increases constantly up to ca. 15 km (crystallization pressure > 2 - 4 kbar). During the last glacial maximum, the ELA was ca. 550 m lower than today in the Southern Andes (Hulton et al., 1994). This lowering of the ELA during the last glacial maximum increased the glaciated area by ca. 20 % in subarea 1 to ca. 35% in subarea 6 (Fig. 3.7 a). Thus erosion during glacial maxima may have been 1/5 to 1/3 more effective than today.

3.5.2 Tectonic versus climatic control on uplift

The strong correlation of climatic, topographic, erosion, and exhumation gradients suggest that climate is a primary factor controlling differential exhumation in the Southern Andes. But to which extent has been exhumation an isostatic response to erosion and how significant has been tectonic uplift?

Both tectonic uplift (by crustal thickening) and isostatic uplift (due to erosional unloading) act on a spatial scale of 10^3 - 10^4 km^2 and a time scale of about 10^4 years (e.g. Cathless, 1975). Consequently, even rapid rates of regional erosion (several mm/a over an area of several thousands of kilometers) do not cause the surface (determined by the mean elevation of an area) to depart from its isostatically balanced level by more than a few tens of meters (England and Molnar, 1990). It is clear from observing the mean elevations in the Southern Andes (Fig. 3.3 a) and comparing these with the exhumation pattern (Fig. 3.7 b) that zones of high rock uplift/exhumation do not correspond with zones of high mean elevation. Instead high rock uplift/exhumation rates correspond to zones of low mean elevation. This suggests that rock uplift is controlled significantly by erosion.

Assuming that the observed southward decrease of mean elevation may is completely the result of higher rates of erosion, the rock uplift induced by erosional unloading can be constrained. Due to isostatic compensation, the change in mean elevation resulting from erosional unloading is usually a small fraction (10 – 20 %) of the associated exhumation (e.g. Tsuboi, 1983). Fig. 3.8 shows the effect of erosional unloading on topography and rock uplift/exhumation in the study area using an isostatic compensation model: Along strike of the Main Cordillera, the mean elevation decreases from ca. 1200 m at 37°S to ca. 700 m at 43°S whereas the level of erosion increases from less than 3 km to 15 km.

In Fig. 3.8, the amount of erosion necessary to produce the lowering of the mean surface along strike of the study area equals the difference between the mean elevation and the uplifted surface for each 1°-latitude increment. Note that the uplifted surface is

only a hypothetical surface which does not exist in reality. Moreover, the uplifted surface is a conceptual surface representing the level of exhumation attributed to erosional unloading.

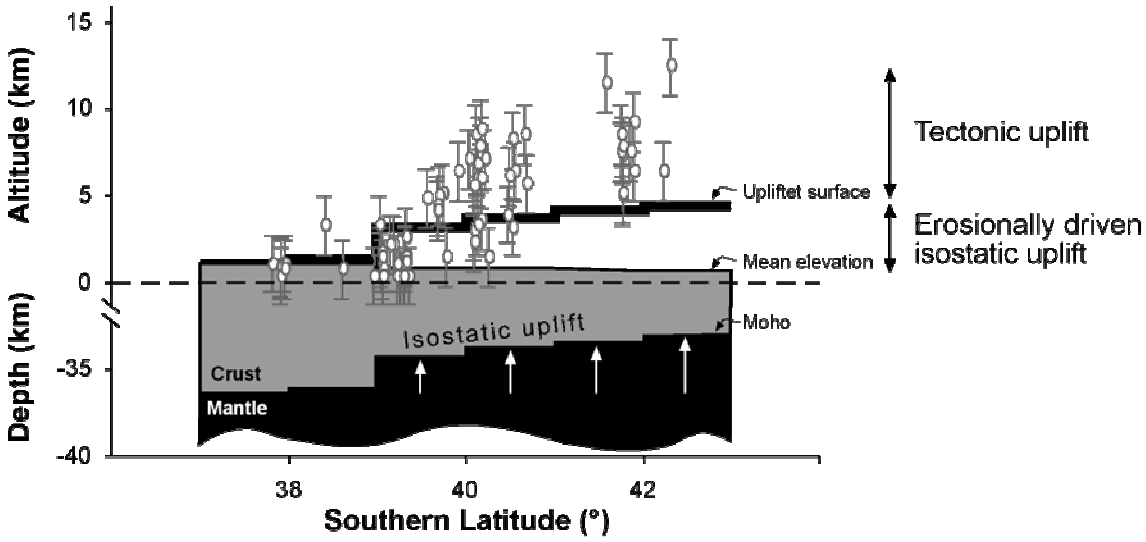

Fig 3.8: *Effect of erosionally driven isotopic uplift in the Southern Andes (superposed is the relative variation of the level of exhumation indicated by crystallization depths (grey dots with error bars) of granitoids of the NPB inferred from Al-in-hbl geothermobarometry, data from Seifert et al., in press).*

According to this model, erosionally driven differential uplift vary from 0 km at 37-38°S (which is by definition the reference level) to about 4 km at 42-43°S. From the comparison of the erosionally driven differential uplift with the differential exhumation pattern, the relative importance of climatically and tectonically controlled rock uplift can be constrained: Whereas north of ca. 40°S, the level of exhumation is at or below the uplifted surface, to the South, the level of exhumation is significantly above the uplifted surface. In other words, exhumation in the northern part of the study area can be explained exclusively by erosionally driven isostatic uplift whereas exhumation in the southern part of the study area requires a significant amount of tectonic uplift. The relative importance of climatically controlled uplift/exhumation can be expressed by the ratio

$$Up_E / (Up_E + Up_T)$$

where Up_E is the erosionally driven isostatic uplift and Up_T the tectonic uplift, and ranges from 1 (in the north) to about 1/3 (in the south).